

The Magnetic Properties of Nickel(II) 2,2-Dimethylpropanoate Dimers and the Crystal Structure of Di-2,4-lutidinetetrakis(μ -2,2-dimethylpropanoato)dinickel(II)

Nobuchika Hirashima,^a Steinar Husebye,^{b,*} Michinobu Kato,^c Knut Maartmann-Moe,^b Yoneichiro Muto,^a Michio Nakashima^a and Tadashi Tokii^a

^aDepartment of Chemistry, Faculty of Science and Engineering, Saga University, Saga 840, Japan, ^bDepartment of Chemistry, University of Bergen, N-5007 Bergen, Norway and ^cDepartment of Chemistry, Aichi Prefectural University, Mizuho-ku, Nagoya 467, Japan

Hirashima, N., Husebye, S., Kato, M., Maartmann-Moe, K., Muto, Y., Nakashima, M. and Tokii, T., 1990. The Magnetic Properties of Nickel(II) 2,2-Dimethylpropanoate Dimers and the Crystal Structure of Di-2,4-lutidinetetrakis(μ -2,2-dimethylpropanoato)dinickel(II). – *Acta Chem. Scand.* 44: 984–989.

Three dimeric Ni(II) 2,2-dimethylpropanoate complexes, $[\text{Ni}(\text{Me}_3\text{CCOO})_2\text{L}]_2$, where L = 2-ethylpyridine, 2,4-lutidine (2,4-lu) and 2,5-lutidine, and the corresponding 2-ethylbutanoate complex with L = quinoline, have been prepared. All these complexes display a dimer type of antiferromagnetism. For the 2,4-lutidine complex, a change in magnetic properties at ca. 200 K is observed, indicating a phase transition. The structure of this complex at 22 °C was determined by X-ray crystallography. Unit cell parameters for $[\text{Ni}(\text{Me}_3\text{CCOO})_2(2,4\text{-lu})]_2$ are $a = 9.846(1)$, $b = 10.735(1)$, $c = 11.215(1)$ Å, $\alpha = 116.40(1)$, $\beta = 101.86(1)$, $\gamma = 98.65(1)^\circ$, $Z = 1$. The green crystals are triclinic, space group $P1$. Based on 4236 observed reflections, the structure was refined to a conventional R -value of 0.048. The compound has the dimeric structure found in numerous copper acetate adducts. Thus nickel has a square pyramidal coordination with an axial 2,4-dimethylpyridine ligand and four basal oxygens, one from each of the 2,2-dimethylpropanoate ligands. The Ni...Ni separation in the dimer is 2.7080(5) Å.

Although a large number of dimeric copper(II) carboxylates have been prepared and characterized, very few nickel(II) complexes analogous to the copper(II) dimers have been reported. The structure of the dimeric nickel(II) 2,2-dimethylpropanoate adduct with quinaldine, $[\text{Ni}(\text{Me}_3\text{CCOO})_2(\text{quinaldine})]_2$, has recently been determined by Kirillova *et al.* and found to be a copper(II) acetate monohydrate type of dimeric structure.¹ An antiferromagnetic exchange integral of $J = -160 \text{ cm}^{-1}$ has been reported for this complex.¹ The J values for nickel(II) 2,2-dimethylpropanoate adducts with pyridine, α -picoline, γ -picoline, quinoline and triphenylphosphine (-150 to -157 cm^{-1})² and the nickel benzoate adduct with quinoline (-125 cm^{-1})³ have also been evaluated.

We have now been able to prepare three nickel(II) 2,2-dimethylpropanoate complexes, $[\text{Ni}(\text{Me}_3\text{CCOO})_2\text{L}]_2$, where L = 2-ethylpyridine (2-ety), 2,4-lutidine (2,4-lu) and 2,5-lutidine (2,5-lu), and the nickel(II) 2-ethylbutanoate adduct with quinoline, $[\text{Ni}(\text{Et}_2\text{CHCOO})_2(\text{quin})]_2$. These complexes all display a dimer type of antiferromagnetism. Among them, $[\text{Ni}(\text{Me}_3\text{CCOO})_2(2,4\text{-lu})]_2$ has shown remarkable change at ca. 200 K in the susceptibility–temperature curve, suggesting the occurrence of a phase transition. Hence, the crystal structure of the 2,4-lutidine

adduct was determined by X-ray diffraction in order to study magneto-structural correlations.

Experimental

Syntheses. The starting material, $\text{Ni}(\text{Me}_3\text{CCOO})_2(\text{Me}_3\text{CCOOH})_2$, was prepared as follows. Basic nickel(II) carbonate (5 mmol) was mixed with 2,2-dimethylpropanoic acid (30 mmol). When the mixture was warmed gently, a green solid was formed with the evolution of carbon dioxide. The product was dissolved in benzene (150 ml) and the solution was concentrated to one-third of its volume. When petroleum ether was added to the solution, green crystals precipitated. After washing with petroleum ether, the crystals were dried *in vacuo* at room temperature.

To prepare $[\text{Ni}(\text{Me}_3\text{CCOO})_2\text{L}]_2$ (L = 2-ety, 2,4-lu and 2,5-lu) a solution of L (4 mmol) in toluene (5 ml) was added to a solution of $\text{Ni}(\text{Me}_3\text{CCOO})_2(\text{Me}_3\text{CCOOH})_2$ (2 mmol) in toluene (30 ml). After the solution had been concentrated to one-third of its original volume, it was allowed to stand overnight at ca. 5 °C in a refrigerator. The separated green crystals were collected, washed with petroleum ether and dried *in vacuo* at room temperature. Yield: ca. 0.5 g for each of these three adducts.

$[\text{Ni}(\text{Et}_2\text{CHCOO})_2] \cdot \text{H}_2\text{O}$ was prepared from 2-ethyl-

* To whom correspondence should be addressed.

Table 1. Magnetic parameters and magnetic moments.

Complex	J/cm^{-1}	g	$N\alpha/10^{-6} \text{ emu}$	$10^2 P$	$10^2 \sigma_{\text{dis}}$	$\mu_{\text{eff}}/\text{B.M.}$	T/K
$[\text{Ni}(\text{Me}_3\text{CCOO})_2(2\text{-etpy})]_2$	-221	2.85	280	0.82	1.52	2.11	302
$[\text{Ni}(\text{Me}_3\text{CCOO})_2(2,4\text{-lu})]_2$							
Low-T region	-194	2.40	275	0.26	1.41		
High-T region	-224	2.72	202	0.02	3.89	2.00	297
$[\text{Ni}(\text{Me}_3\text{CCOO})_2(2,5\text{-lu})]_2$	-128	2.38	260	2.48	0.90	2.34	298
$[\text{Ni}(\text{Et}_2\text{CHCOO})_2(\text{quin})]_2$	-216	2.35	276	1.28	1.95	1.72	284

butanoic acid and basic nickel(II) carbonate in the same way as the preparation of $[\text{Ni}(\text{Me}_3\text{CCOO})_2(\text{Me}_3\text{CCOOH})_2]$.

In the case of $[\text{Ni}(\text{Et}_2\text{CHCOO})_2(\text{quin})]_2$, mixtures of $[\text{Ni}(\text{Et}_2\text{CHCOO})_2] \cdot \text{H}_2\text{O}$ (3 mmol) and quinoline (2.7 mmol) in toluene (30 ml) were stirred for about 30 min at room temperature. The resultant solution was filtered and concentrated to one-third of the volume. When petroleum ether was added to the solution, green crystals precipitated. They were washed with petroleum ether and dried *in vacuo* at room temperature. Yield: ca. 0.7 g.

Magnetic measurements. Magnetic susceptibilities in the temperature range 80–300 K were determined by the Faraday method. The correction for diamagnetic contribution was made by use of Pascal's constants.⁴ The cryomagnetic data were analyzed by using eqn. (1), based on the ex-

$$\chi_A = \frac{2Ng^2\beta^2}{3kT} [1 + \frac{1}{3} \exp(-2J/kT)]^{-1} (1 - P) + \frac{2Ng_i^2\beta^2}{3kT} P + N\alpha \quad (1)$$

change channel model developed by Rakitin *et al.*,⁵ where P is the mole fraction of the noncoupled paramagnetic nickel(II) impurity, g_i is the average g factor for the impurity, and the other symbols have their usual meanings. A fixed value of 2.2 was used for g_i . The best-fit parameters for J , g , P and $N\alpha$ were obtained by a nonlinear least-squares fitting procedure. The quantity of fit was estimated by means of a discrepancy index, $\sigma_{\text{dis}} = [\sum(\chi_{\text{obsd}} - \chi_{\text{calcd}})^2 / \sum\chi_{\text{obsd}}^2]^{1/2}$. Effective magnetic moments at room temperature were calculated from eqn. (2). The thermal magnetic

$$\mu_{\text{eff}} = 2.83 [(\chi_A - N\alpha)T]^{1/2} \quad (2)$$

data are shown in Figs. 1 and 2 as plots of χ_A vs. T . The values of J , g , $N\alpha$, P , σ_{dis} and μ_{eff} are summarized in Table 1.

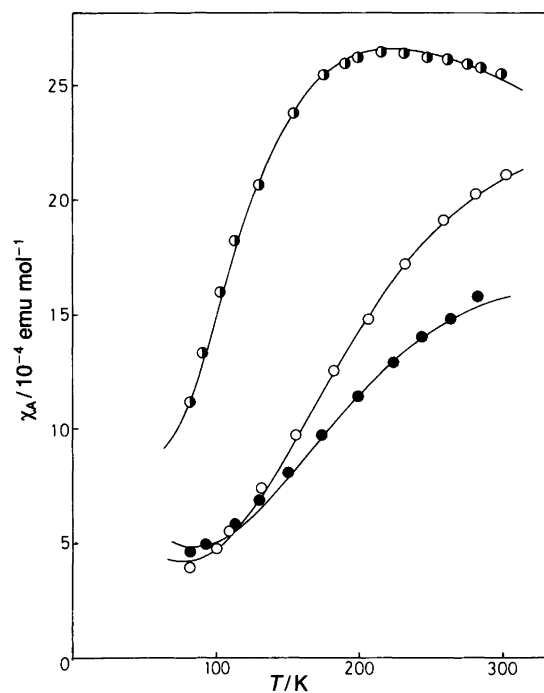


Fig. 1. Variation of magnetic susceptibilities with temperature. (●) $[\text{Ni}(\text{Me}_3\text{CCOO})_2(2,5\text{-lu})]_2$, (○) $[\text{Ni}(\text{Me}_3\text{CCOO})_2(2\text{-etpy})]_2$, (●) $[\text{Ni}(\text{Et}_2\text{CHCOO})_2(\text{quin})]_2$. The solid curves were obtained as described in the text.

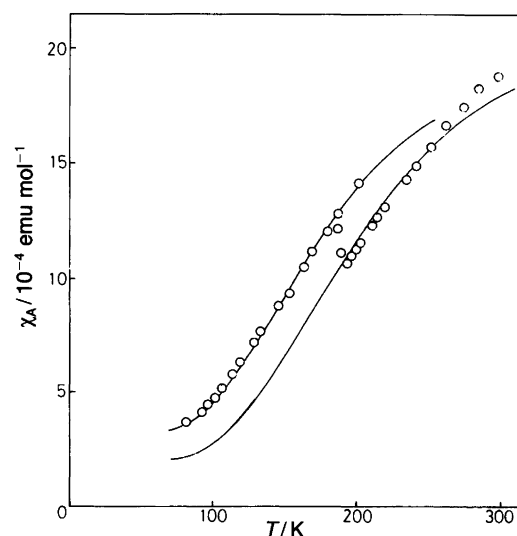


Fig. 2. Variation of magnetic susceptibilities with temperature. (○) $[\text{Ni}(\text{Me}_3\text{CCOO})_2(2,4\text{-lu})]_2$. The solid curves were obtained as described in the text.

X-Ray data. Data collection was carried out at 22 °C using graphite monochromated Mo K α radiation. Attempted data collection at low temperatures resulted in cracking of the crystals and a total loss of intensity. Unit cell parameters are based on least-squares fits to the diffractometer settings of 25 general reflections. Intensity data were recorded using ω -scans, a constant scan rate of 4° min⁻¹ and a minimum scan width of 1.50°, including background scans of 0.25° at the beginning and the end of each scan. The orientation of the crystal was checked at intervals of 500 recordings and the intensities of three standard reflections were checked every 3 h. Corrections were applied to the reflection intensities based on a small variation (<4%) in the intensities of the standard reflections.

The structure was solved by direct methods and refined by full-matrix least-squares iterations. The function minimized is $\Sigma w(\Delta F)^2$. Weights were calculated according to $w = \{[\sigma(I)]^2 + (0.040F^2)^2\}^{-1}$. Non-hydrogen atoms were refined anisotropically. Hydrogen atoms were placed in calculated positions (C–H = 0.95 Å) with isotropic temperature factors set equal to 1.3 times the isotropic temperature factors of the carbon atoms to which they were bonded. The temperature factors of the methyl groups on the acetate ligands are very high and may indicate some disorder. However, the final difference map showed no maxima higher than $-0.47 \text{ e } \text{Å}^{-3}$. Refinement was terminated when parameter shifts became less than 1% of the associated standard deviations. Computer programs used were supplied by Enraf–Nonius (SPD/VAX V 3.0). Crystal and experimental data are summarized in Table 2.

Table 2. Crystal and experimental data.

Compound	[Ni(Me ₃ CCOO) ₂ (2,4-lu)] ₂
Diffractometer	Enraf–Nonius CAD-4
Radiation	Mo K α
Wavelength/Å	0.710 73
Crystal system	Triclinic
<i>a</i> /Å	9.846(1)
<i>b</i> /Å	10.735(1)
<i>c</i> /Å	11.215(1)
α /°	116.40(1)
β /°	101.86(1)
γ /°	98.65(1)
<i>V</i> /Å ³	998.8
Space group	<i>P</i> 1 (No. 2)
Formula weight	736.2
<i>Z</i>	1
<i>D</i> _{calc} /g cm ⁻³	1.224
μ (Mo K α)/cm ⁻¹	9.90
Crystal dimensions/mm	0.29×0.29×0.25
Scan mode/max. θ /°	ω -scan/30
Fudge factor	0.040
Scale factor	0.5175
No. of independent measurements	5785
No. with $I > 2\sigma$	4236
Transmission factors	0.759–0.952
$R = \Sigma F_o - F_c /\Sigma F_o$	0.048
$R_w = [\Sigma w(F_o - F_c)^2/\Sigma w F_o^2]^{0.5}$	0.057
$S = [\Sigma w(\Delta F)^2/N-n]^{0.5}$	1.733

Results and discussion

Atomic positional parameters are listed in Table 3, bond distances and angles in Table 4 and molecular planes and interplanar angles in Table 5. Complementary data are available from one of the authors (K.M.-M.).

Nickel coordination. Fig. 3 shows the structure of the dimeric molecule and the labelling of the atoms. The four 2,2-dimethylpropanoate ligands are all bridging. Each nickel atom has a distorted square pyramidal coordination, with a 2,4-lutidine ligand in an axial position while the acetate oxygens are basal. This is the classical structure found in the analogous copper acetate dimers. The coordination sphere of nickel is shown in Fig. 4. The dimeric molecules are centrosymmetric; the packing of the molecules in the unit cell is shown in Fig. 5. The Ni–Ni distance in the molecule is 2.7080(5) Å, and Ni is located 0.251 Å above the plane through the four basal oxygens. The average Ni–O bond length is 2.006(9) Å and Ni–N is 2.035(2) Å. Corresponding values in the analogous [Ni(Me₃CCOO)₂(quinaldine)]₂ dimer are 2.754(3), 0.23, 2.01 and 2.07 Å.¹ In the monothiocarboxylate complex, [Ni(PhCOS)₂]₂(EtOH), one Ni atom is bonded to five O atoms as well as to the other Ni atom (2.498 Å) in a distorted octahedral arrangement. Here the Ni–O bonds are in the range 2.00–2.09 Å.⁶ There are essentially two

Table 3. Positional parameters and their estimated standard deviations.^a

Atom	<i>x</i>	<i>y</i>	<i>z</i>	<i>B</i> /Å ²
Ni	0.02430(3)	-0.12111(3)	-0.09366(3)	3.552(6)
O11	0.1881(2)	0.0429(2)	-0.0551(2)	5.18(5)
O12	-0.1549(2)	-0.2426(2)	-0.0997(2)	5.16(5)
O21	0.1327(2)	-0.1174(2)	0.0799(2)	5.13(5)
O22	-0.0982(2)	-0.0833(2)	-0.2342(2)	5.07(5)
N	0.0959(2)	-0.2696(2)	-0.2367(2)	4.22(5)
C1	0.1089(3)	-0.3981(3)	-0.2505(3)	5.06(7)
C2	0.1683(3)	-0.4826(3)	-0.3501(4)	6.47(9)
C3	0.2156(3)	-0.4405(4)	-0.4347(3)	6.65(9)
C4	0.2007(3)	-0.3102(4)	-0.4202(3)	6.59(9)
C5	0.1411(3)	-0.2284(3)	-0.3221(3)	5.38(8)
C6	0.0569(4)	-0.4457(3)	-0.1577(4)	7.4(1)
C7	0.2837(4)	-0.5317(5)	-0.5402(4)	10.6(1)
C11	0.2224(3)	0.1772(2)	0.0213(2)	3.91(5)
C12	0.3565(3)	0.2636(3)	0.0159(3)	5.75(8)
C13	0.4804(5)	0.2012(7)	0.0411(7)	16.4(2)
C14	0.3306(6)	0.2408(5)	-0.1282(4)	14.6(2)
C15	0.3964(6)	0.4166(5)	0.1213(5)	17.1(2)
C21	0.1508(3)	-0.0209(2)	0.02021(2)	4.17(6)
C22	0.2493(4)	-0.0294(3)	0.3212(3)	6.18(8)
C23	0.2725(5)	-0.1788(4)	0.2738(4)	9.4(1)
C24	0.3974(5)	0.0713(5)	0.3570(5)	14.6(2)
C25	0.2005(6)	0.0211(6)	0.4422(4)	18.2(2)

^aNon-hydrogen atoms are refined anisotropically and are represented by their equivalent isotropic thermal parameters defined as: $(4/3)[a^2\beta(1,1) + b^2\beta(2,2) + c^2\beta(3,3) + ab(\cos \gamma)\beta(1,2) + ac(\cos \beta)\beta(1,3) + bc(\cos \alpha)\beta(2,3)]$.

Table 4. Interatomic distances (in Å) and angles (in °).^a

Distances			
Ni...Ni'	2.7080(5)	C21-O22'	1.242(3)
Ni-O11	2.017(1)	C21-C22	1.528(3)
Ni-O12	1.999(2)	C22-C23	1.519(4)
Ni-O21	1.998(1)	C22-C24	1.535(5)
Ni-O22	2.010(1)	C22-C25	1.434(5)
Ni-N	2.035(2)	N-C1	1.348(3)
C11-O11	1.250(2)	C1-C2	1.393(3)
C11-O12'	1.241(2)	C2-C3	1.350(4)
C11-C12	1.523(3)	C3-C4	1.369(4)
C12-C13	1.513(6)	C4-C5	1.374(3)
C12-C14	1.483(5)	C5-N	1.342(3)
C12-C15	1.462(5)	C1-C6	1.489(4)
C21-O21	1.252(3)	C3-C7	1.517(4)
Bond angles			
O11-Ni-O21	89.02(7)	C1-C2-C3	122.4(3)
O11-Ni-O22	88.68(7)	C2-C3-C4	116.9(2)
O12-Ni-O21	89.95(7)	C3-C4-C5	120.0(3)
O12-Ni-O22	88.76(7)	C4-C5-N	123.0(3)
O11-Ni-O12	165.46(6)	N-C1-C6	118.0(2)
O21-Ni-O22	165.74(6)	C2-C1-C6	122.0(2)
O11-Ni-N	91.81(6)	C2-C3-C7	121.9(3)
O12-Ni-N	102.65(6)	C4-C3-C7	121.2(3)
O21-Ni-N	99.97(7)	C11-C12-C13	108.7(3)
O22-Ni-N	94.17(7)	C11-C12-C14	108.4(2)
O11-C11-O12'	124.3(2)	C11-C12-C15	111.9(2)
O11-C11-C12	116.7(2)	C13-C12-C14	105.9(4)
O12'-C11-C12	119.0(2)	C13-C12-C15	109.1(4)
O21-C21-O22'	125.2(2)	C14-C12-C15	112.6(4)
O21-C21-C22	117.4(2)	C21-C22-C23	112.0(2)
O22'-C21-C22	117.4(2)	C21-C22-C24	105.0(2)
Ni-N-C1	127.9(2)	C21-C22-C25	111.5(3)
Ni-N-C5	114.4(1)	C23-C22-C24	105.4(3)
C1-N-C5	117.7(2)	C23-C22-C25	113.2(3)
N-C1-C2	120.0(3)	C24-C22-C25	109.3(4)

^aPrimes denote atoms related to those in Table 3 by a molecular centre of symmetry (0,0,0).

types, A and B, of quadruply bridged dinuclear Ni complexes. A may be represented by the present investigation, where the bridging ligand is a carboxylate group. Such compounds are rare. Type B is more common and has dithiocarboxylate or diamino groups as bridging ligands.⁷⁻⁹ In the A complexes, Ni is five-coordinated and in a square pyramidal environment and there is no Ni-Ni bond. In B complexes there is a Ni-Ni bond, and at approximately right angles to this bond, each Ni is bonded to four ligand atoms (S or N) in a square-planar fashion. In several of these complexes, a sixth, weak Ni-L interaction is taking place. This results in a distorted octahedral environment for Ni.⁸ Also, the Ni-Ni bonding in B complexes results in Ni being displaced more than 0.1 Å out of the basal plane towards the other nickel atom: the opposite is found in the A type complexes.^{1,7,8}

In the carboxylate ligands, the average C-O, C-C and C-CH₃ bond lengths are 1.246, 1.526 and 1.491 Å, respectively. The low average value of the C-CH₃ bond lengths, 1.491 Å as compared to the sum of the covalent radii of 1.54 Å,¹⁰ is probably due to the high degree of thermal movement of the methyl groups. In the 2,4-dimethylpyridine ligand, average C-N and C-C bond lengths in the ring are normal at 1.345 and 1.372 Å.

There is a strong steric interaction between the α -methyl (C6) group of the substituted pyridine ligand and O12 and O21: O12-C6 = 3.192(3) Å and O21-C6 = 3.181(3) Å, as compared to 3.40 Å, the sum of the respective van der Waals radii.⁶ This interaction moves C6 (and thereby the whole ligand) away, so that angle Ni-N-C1 becomes 13.5° larger than angle Ni-N-C5. This effect is seen in the Ni...Ni-N angle of 166.63(5)°. The angles between the carboxyl groups are close to 90°, and the two NiO₄ groups are eclipsed.

Magnetic properties. The magnetic susceptibility data observed for [Ni(Me₃CCOO)₂(2-etpy)]₂, [Ni(Me₃CCOO)₂(2,5-lu)]₂ and [Ni(Et₂CHCOO)₂(quin)]₂ could not be fitted

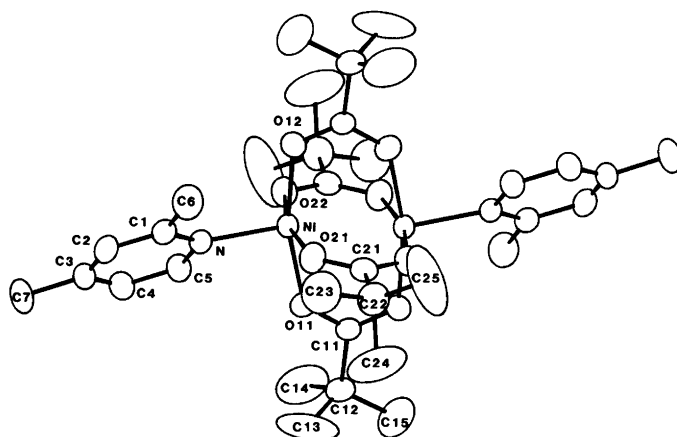


Fig. 3. The structure of the centrosymmetric dimer.

Table 5. Least-squares planes.

No. of plane	Atoms involved	$\Delta_{\max}^a/\text{\AA}$	Distance from plane / \AA	Dihedral angles / $^\circ$
1	O11, O12, O21, O22	0.003	Ni, 0.251	1,5: 84.82(5)
2	Ni, O11, O12', C11, C12	0.025	C13, -1.099; C14, 1.280; C15, -0.134	2,3: 89.44(7)
3	Ni, O21, O22', C21, C22	0.053	C23, -0.336; C24, 1.544; C25, -0.679	2,4: 42.40(7)
4	Ni, N, C1-C7	0.065		3,4: 129.93(9)
5	N, C1-C7	0.013	Ni, 0.140	4,5: 1.14(2.1)

^aMaximum deviation of any of the atoms involved from the plane. Planes 2 and 3 are restricted to pass through the centre of the dimer.

satisfactorily to the magnetic susceptibility equation, eqn. (3), for the coupling of two $S = 1$ states. However, a

$$\chi_A = \frac{N\beta^2 g^2}{kT} \left(\frac{5 + \exp(-4J/kT)}{5 + 3 \exp(-4J/kT) + \exp(-6J/kT)} \right) + N\alpha \quad (3)$$

good fit to eqn. (1) was obtained for the magnetic data (Fig. 1 and Table 1). As can be seen in Fig. 2, an interesting change in the susceptibility-temperature curve of $[\text{Ni}(\text{Me}_3\text{CCOO})_2(2,4\text{-lu})_2]_2$ was observed at ca. 200 K. The magnetic susceptibilities observed in upper (200–300 K) and lower (80–200 K) regions with respect to the transition temperature are well reproduced by eqn. (1) using the appropriate parameters listed in Table 1. For the exchange channels between unpaired electrons on the metal ions in dimeric nickel(II) carboxylates, Rakitin *et al.*⁵ proposed two superexchange channels of $d_{x^2-y^2}-\sigma_{\text{O}}-\sigma_{\text{C}}-\sigma_{\text{O}}-d_{x^2-y^2}$ (σ -path) and $d_{xy}-\pi_{\text{O}}-\pi_{\text{C}}-\pi_{\text{O}}-d_{xy}$ (π -path), whereas Bencini *et al.*³ suggested two direct ones of $d_{x^2-y^2}-d_{x^2-y^2}$ (δ -bonding) and $d_{z^2}-d_{z^2}$ (σ -bonding). Kirillova *et al.*¹ claimed the absence of a direct Ni(II)–Ni(II) bond in $[\text{Ni}(\text{Me}_3\text{CCOO})_2(\text{quinaldine})]_2$ by the fact that the Ni(II)–Ni(II) distance (2.753 \AA) is considerably longer than that in the diamagnetic nickel(II) phenylthioacetate

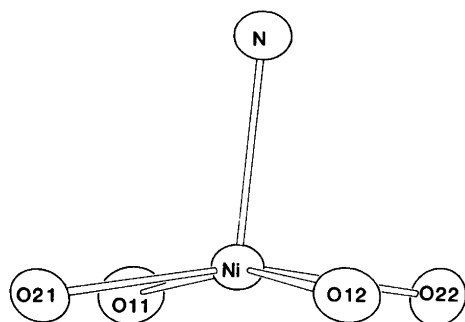


Fig. 4. The square-pyramidal coordination of Ni(II).

dimer (2.551 \AA).⁷ In the present study the Ni(II)–Ni(II) distance is 2.708 \AA , a value quite similar to that found in $[\text{Ni}(\text{Me}_3\text{CCOO})_2(\text{quinaldine})]_2$.¹ At present, however, magnetic and structural data on nickel(II) carboxylate dimers are too sparse to distinguish between the different proposals above. Recently, Uekusa *et al.* have shown that the Cu–Cu distances in copper(II) formate adducts with larger singlet–triplet separations (ca. 500 cm^{-1}) are definitely longer than those found in the corresponding copper(II) acetates with smaller singlet–triplet separations (ca. 300 cm^{-1}).¹¹ The results confirm the early proposal by Goodgame *et al.* that the spin–spin coupling in copper(II) carboxylate dimers is mainly due to the superexchange interaction through the carboxylate bridges, rather than a metal–metal direct interaction.¹² At the present stage, a wide range of comparative magneto-structural studies on both Cu(II) and Ni(II) carboxylate dimeric systems are required to give deeper insight into the spin–spin coupling mechanism in these systems. Such comparative studies are now in progress.

It may be noted here that the σ_{dis} values shown in Table 1 are somewhat higher than those reported previously for corresponding copper(II) 2,2-dimethylpropanoate dimers, $(4-9) \times 10^{-3}$.¹³ This may be due to the neglect of effects associated with the zero-field splitting of individual nickel(II) ions.¹⁴

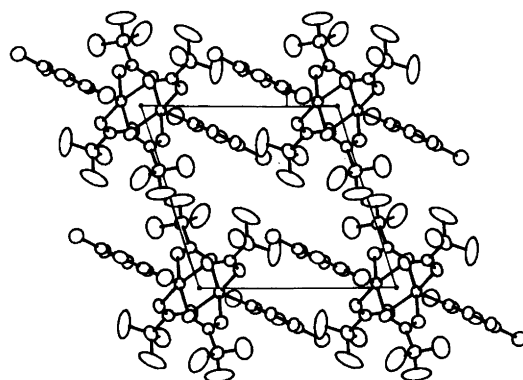


Fig. 5. The packing of the dimers in the unit cell.

References

1. Kirillova, N. I., Struchkov, Yu. T., Porai-Koshits, M. A., Pasynskii, A. A., Antsyshkina, A. S., Minacheva, L. Kh., Sadikov, G. G., Idrisov, T. Ch. and Kalinnikov, V. T. *Inorg. Chim. Acta* 42 (1980) 115.
2. Novotortsev, V. M., Rakitin, Yu. V., Pasynskii, A. A. and Kalinnikov, V. T. *Dokl. Acad. Nauk SSSR* 240 (1978) 335.
3. Bencini, A., Benelli, C., Gatteschi, D. and Zanchini, C. *J. Am. Chem. Soc.* 102 (1980) 5820.
4. Selwood, P. W. *Magnetochemistry*, Interscience, New York 1956, pp. 78 and 91.
5. Rakitin, T. V., Kalinnikov, V. T. and Eremin, M. V. *Theor. Chim. Acta* 45 (1977) 167.
6. Bonamico, M., Dessy, G. and Fares, V. *J. Chem. Soc., Chem. Commun.* (1969) 697.
7. Bonamico, M., Dessy, G. and Fares, V. *J. Chem. Soc., Dalton Trans.* (1977) 2315.
8. Bellitto, C., Dessy, G. and Fares, V. *Inorg. Chem.* 24 (1985) 2815.
9. Cotton, F. A., Matusz, M. and Poli, R. *Inorg. Chem.* 26 (1987) 1472.
10. Pauling, L. *Nature of the Chemical Bond*, 3rd. ed., Cornell University Press, New York 1960.
11. Uekusa, H., Ohba, S., Saito, Y., Kato, M., Tokii, T. and Muto, Y. *Acta Crystallogr., Sect. C* 45 (1989) 377.
12. Goodgame, D. M. L., Hill, N. J., Marsham, D. F., Skapski, A. C., Smart, M. L. and Troughton, P. G. H. *Chem. Commun.* (1969) 629.
13. Muto, Y., Hirashima, N., Tokii, T., Kato, M. and Suzuki, I. *Bull. Chem. Soc. Jpn.* 59 (1986) 3672.
14. Ginsberg, A. P., Martin, R. L., Brookes, R. W. and Sherwood, R. C. *Inorg. Chem.* 11 (1972) 2884.

Received February 26, 1990.